Numerical Validation of a Boundary Element Method with Electric Field and Its Normal Derivative as the Boundary Unknowns*

Johannes Markkanen[1], Alex J. Yuffa[2], and Joshua A. Gordon[2]

[1]Max Planck Institute for Solar System Research, Göttingen, 37077, Germany
markkanen@mps.mpg.de

[2]National Institute of Standards and Technology, Boulder, CO 80305, USA
alex.yuffa@nist.gov, josh.gordon@nist.gov

Abstract – We recently developed a surface integral equation method where the electric field and its normal derivative are chosen as the boundary unknowns. After reviewing this formulation, we present preliminary numerical calculations that show good agreement with the known results. These calculations are encouraging and invite the further development of the numerical solution.

Index Terms – Boundary element method, electromagnetic scattering, surface integral equations.

I. INTRODUCTION

We have recently formulated a frequency domain surface integral equation method [1] that is applicable to penetrable closed surface scatterers. The method has several unique applications and advantages over the standard Stratton–Chu formulation as discussed in [1]. In our formulation, we choose the electric field (E-field) and its normal derivative as the boundary unknowns. This choice leads to 12 scalar unknowns on the surface of the scatterer; for each homogeneous region we have three scalar unknowns associated with the E-field and three scalar unknowns associated with its normal derivative. Similar to a typical surface integral equation formulation, our formulation is also based on the Green's theorem (Green's second identity). This formulation leads to *six* scalar equations, and thus it must be supplemented with *six* additional constraints in order to have the same number of equations as unknowns. Three of these constraints come from the well-known continuity condition of the E-field across an interface and the other three come from the recently derived continuity condition for the normal derivative of the E-field [1–3].

In this paper, we numerically solve the above discussed equations for several scatterers and compare our results to the results obtained via other methods. We also comment on the choice of the basis functions in the Galerkin's method and its effects on numerical convergence.

II. FORMULATION REVIEW

Consider a scatterer with permittivity $\overset{2}{\epsilon}$ and permeability $\overset{2}{\mu}$. The space surrounding the scatterer is assumed to be lossless with permittivity $\overset{1}{\epsilon}$ and permeability $\overset{1}{\mu}$, i.e., $\{\overset{1}{\epsilon},\overset{1}{\mu}\}\in\mathbb{R}$. If we apply the Green's second identity to the scatterer and the surrounding space, then, after setting the observation point on the surface of the scatterer, we obtain:

$$\overset{\text{inc}}{\boldsymbol{E}}(\widetilde{S}) - -\!\!\!\!\!\!\int_{\Sigma}\left[\overset{1}{G}\,\frac{\partial\overset{1}{\boldsymbol{E}}}{\partial N} - \overset{1}{\boldsymbol{E}}\,\frac{\partial\overset{1}{G}}{\partial N}\right]\mathrm{d}S = \frac{1}{2}\overset{1}{\boldsymbol{E}}(\widetilde{S}), \tag{1a}$$

and

$$-\!\!\!\!\!\!\int_{\Sigma}\left[\overset{2}{G}\,\frac{\partial\overset{2}{\boldsymbol{E}}}{\partial N} - \overset{2}{\boldsymbol{E}}\,\frac{\partial\overset{2}{G}}{\partial N}\right]\mathrm{d}S = \frac{1}{2}\overset{2}{\boldsymbol{E}}(\widetilde{S}), \tag{1b}$$

where $\overset{\text{inc}}{\boldsymbol{E}}$ is the incident E-field, $-\!\!\!\!\!\int$ denotes the Cauchy principal value integral, Σ denotes the surface of the scatterer, $\frac{\partial}{\partial N}$ denotes the normal derivative, G is the free-space Green's function, and $\widetilde{S}$ is the observation point on Σ. In (1), the overset digit indicates if the quantity is associated with the scatterer or the surrounding space, e.g., $\overset{2}{\boldsymbol{E}}$ is the E-field just inside the scatterer. In the Gaussian unit system, the continuity condition for the E-field across an interface can be written as [1]:

$$\overset{2}{\boldsymbol{E}} = \overset{\text{r}}{\epsilon}^{-1}\left(\boldsymbol{N}\cdot\overset{1}{\boldsymbol{E}}\right)\boldsymbol{N} + \left(\boldsymbol{S}^{\alpha}\cdot\overset{1}{\boldsymbol{E}}\right)\boldsymbol{S}_{\alpha}, \tag{2a}$$

and the continuity condition for its normal derivative as [1]:

$$\frac{\partial\overset{2}{\boldsymbol{E}}}{\partial N} = \overset{\text{r}}{\mu}\left(\frac{\partial\overset{1}{\boldsymbol{E}}}{\partial N} - \nabla^{\alpha}\left[\left(\boldsymbol{N}\cdot\overset{1}{\boldsymbol{E}}\right)\boldsymbol{S}_{\alpha} - \left(\boldsymbol{S}_{\alpha}\cdot\overset{1}{\boldsymbol{E}}\right)\boldsymbol{N}\right]\right) + \nabla^{\alpha}\left[\left(\boldsymbol{N}\cdot\overset{2}{\boldsymbol{E}}\right)\boldsymbol{S}_{\alpha} - \left(\boldsymbol{S}_{\alpha}\cdot\overset{2}{\boldsymbol{E}}\right)\boldsymbol{N}\right], \tag{2b}$$

Submitted On: September 26, 2018
Accepted On: December 28, 2018

where $\overset{r}{\mu} = \overset{2}{\mu} / \overset{1}{\mu}$, $\overset{r}{\epsilon} = \overset{2}{\epsilon} / \overset{1}{\epsilon}$, $\boldsymbol{N}$ is the unit-normal pointing out of the scatterer, $\boldsymbol{S}_\alpha$ is the surface covariant basis [4], and ∇^α is the contravariant surface derivative [4]. Notice that (2) is written in the Einstein summation convention where the Greek indices range from 1 to 2. Substituting (2) into (1b) and using Gauss's theorem in two dimensions yields [1]:

$$\begin{aligned} \frac{1}{2}\overset{2}{\boldsymbol{E}}(\widetilde{S}) = & \fint_\Sigma \left[\overset{r}{\mu}\overset{2}{G}\,\frac{\partial \overset{1}{\boldsymbol{E}}}{\partial N} - \overset{1}{\boldsymbol{E}}\,\frac{\partial \overset{2}{G}}{\partial N} \right] \mathrm{d}S \\ & + \left(\overset{r}{\mu} - \overset{r}{\epsilon}^{-1}\right) \fint_\Sigma \left(\boldsymbol{N}\cdot\overset{1}{\boldsymbol{E}}\right) \boldsymbol{\nabla}\overset{2}{G}\,\mathrm{d}S \\ & + \left(1 - \overset{r}{\mu}\right) \fint_\Sigma \left(\overset{1}{\boldsymbol{E}}\cdot\boldsymbol{\nabla}\overset{2}{G}\right) \boldsymbol{N}\,\mathrm{d}S, \end{aligned} \tag{3a}$$

where

$$\overset{2}{\boldsymbol{E}} = \overset{1}{\boldsymbol{E}} + \left(\overset{r}{\epsilon}^{-1} - 1\right)\left(\boldsymbol{N}\cdot\overset{1}{\boldsymbol{E}}\right)\boldsymbol{N}. \tag{3b}$$

Equations (3) and (1a) form a set of *six* scalar integral equations with *six* scalar unknowns, namely, $\overset{1}{\boldsymbol{E}}$ and $\frac{\partial}{\partial N}\overset{1}{\boldsymbol{E}}$. This is the set of the integral equations that we numerically solve in the next section.

III. NUMERICAL CALCULATIONS

We discretize the scatterers with flat triangular elements and construct a basis for the E-field and its normal derivative. We use piecewise constant basis functions for each component associated with the triangular surfaces. Thus, the number of unknowns is six times the number of the triangular elements. Furthermore, we use Galerkin's method to discretize the equations. In other words, the test and basis functions are identical. It is worth noting that the basis functions *do not* enforce any continuity conditions for the E-field or its normal derivative along the surface. Hence, it is clear that we cannot obtain an optimal convergence rate. Moreover, we anticipate that the sharp wedges may also cause some difficulties. Finding a better set of basis functions is an interesting question for future research.

The integral equation set given by (3) and (1a) contains singular integrals. The gradient of the Green's function has the strongest singularity, and we decompose it into the normal and surface derivative parts. With the help of integration by parts, the latter one reduces to an integral over a triangular surface and a closed integral over the triangle's edges. We evaluate these integrals using the standard singularity extraction technique [5] in which the singular part is calculated analytically and the remaining part is calculated numerically. We solve the resulting system of equations for the boundary unknowns iteratively with the generalized minimal residual GMRES method with the tolerance of 10^{-5}.

To assess the method, we compare the radar cross-section (RCS) of a sphere in free-space meshed by 940 flat triangular patches with the Mie series solution. Figure 1 shows the RCS of a dielectric sphere with $\overset{1}{k}\rho = 1$, $\overset{2}{\epsilon} = 4$, and $\overset{2}{\mu} = 1$, where ρ is the radius of the sphere and Fig. 2 shows the RCS of a lossy sphere with $\overset{1}{k}\rho = 4$, $\overset{2}{\epsilon} = -2 + \mathrm{i}$, and $\overset{2}{\mu} = 1$. From the figures, we see that our solution agrees well with the Mie series solution in both the dielectric case and the lossy case. More specifically, the L^2-norm relative error of the far-field $\|\boldsymbol{E}\|^2$ integrated over a solid angle is 4.832×10^{-3} for Fig. 1 and 9.360×10^{-3} for Fig. 2. In general, the accuracy of the solution depends on the shape, size, electric permittivity, and discretization of the scatterer. The current discretization scheme leads to a less accurate solution with respect the mesh density than the conventional Poggio–Miller–Chan–Harringto–Wu–Tsai (PMCHWT) formulation discretized with the RWG functions. This is not surprising because our basis functions are not the most optimal. This is discussed in more detail in Section IV.

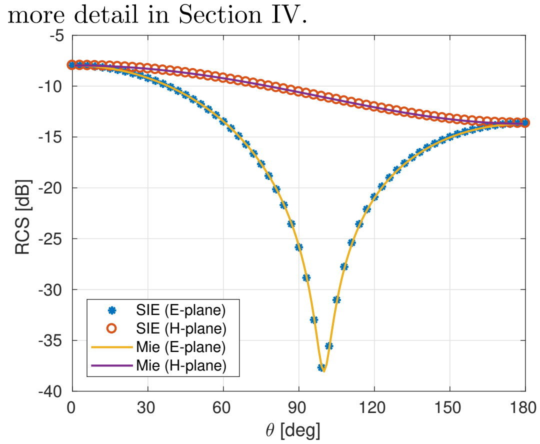

Fig. 1. (Color online) Comparison of the dielectric sphere's RCS as a function of the scattering angle θ computed via the surface integral equation (SIE) method with the Mie series solution.

Next, we investigate the stability of the method with respect to the element size. Because our formulation contains only weakly singular integrals, we expect the condition number of the system matrix to be almost independent of the element size. To demonstrate this, we discretize a cube with and without mesh refinement on edges as shown in Fig. 3. The condition number for the equally triangulated cube equals 117 and for the refined cube it equals 178. In the case of the PMCHWT formulation, the corresponding numbers are 1.0×10^5 and 1.3×10^6, respectively. Hence, the formulation based on the field and its normal derivative is much more stable than the standard surface integral equation formulation without any regularization technique.

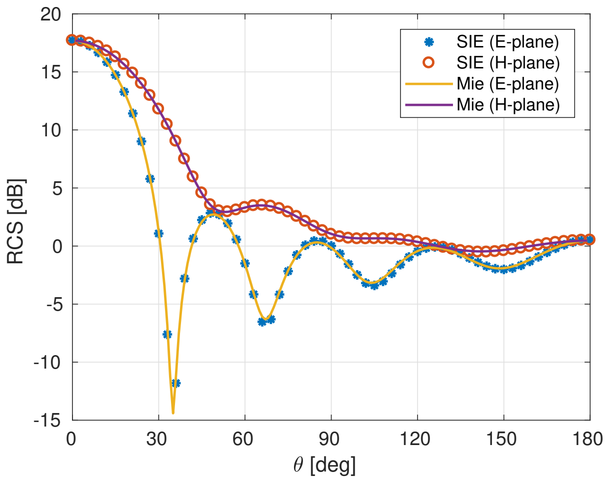

Fig. 2. (Color online) Comparison of the lossy sphere's RCS as a function of the scattering angle θ computed via the surface integral equation (SIE) method with the Mie series solution.

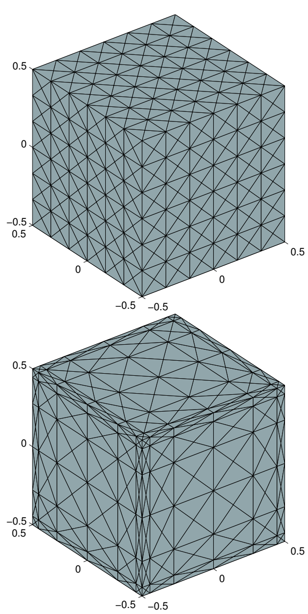

Fig. 3. The discretization of a cube with and without mesh refinements is shown. The condition number associated with the left-hand side cube is 117 and the condition number associated with the right-hand side cube is 178.

Finally, in Fig. 4 we compare the radar cross-section of a dielectric cube computed via our formulation to the standard PMCHWT formulation with the RWG basis and testing functions. We see that the two solutions approach each other with the decreasing element size.

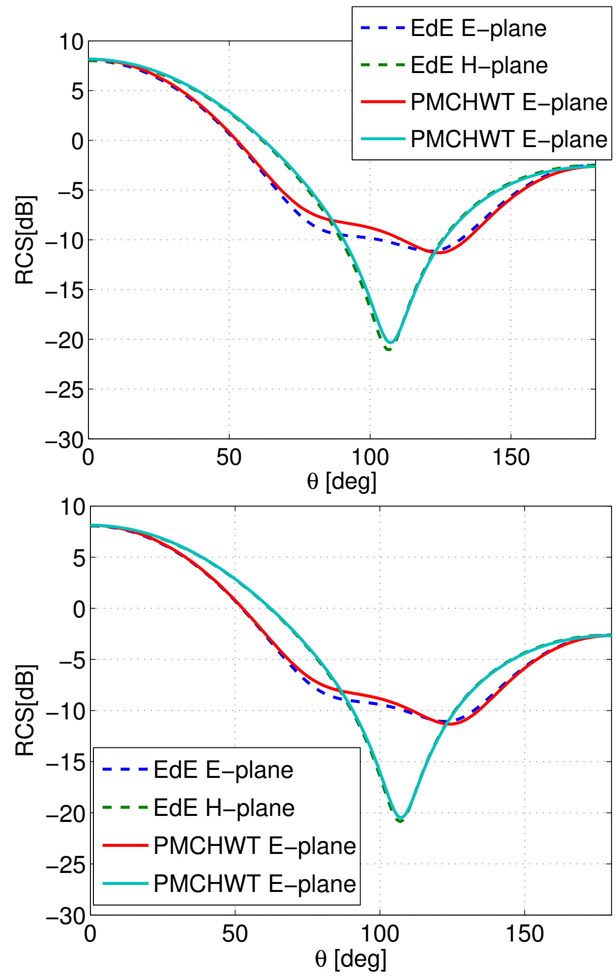

Fig. 4. Scattering by a cube discretized with 432 (top) and 1200 (bottom) triangular elements computed by the new formulation (dash lines) and by the standard PMCHWT formulation (solid lines).

IV. DISCUSSION

We have shown that the discretization scheme using the piecewise constant functions and Galerkin's testing gives a reasonable accuracy for scattering problems involving large and smooth scatterers. However, particularly at low frequencies, the discretization scheme results in low accuracy. This is because we have not exactly enforced the zero divergence condition on the boundary surface. The zero divergence condition can be enforced by requiring that (4) holds on each surface patch. Namely, we require that: [1]

$$\int_{\Pi_i} \boldsymbol{N} \cdot \frac{\partial \boldsymbol{E}}{\partial N} \mathrm{d}S = \int_{\Pi_i} (\boldsymbol{N} \cdot \boldsymbol{E}) W^{\alpha}_{\alpha} \mathrm{d}S - \int_{\partial \Pi_i} n^{\alpha} (\boldsymbol{S}_{\alpha} \cdot \boldsymbol{E}) \mathrm{d}C, \quad (4)$$

where W_α^α is the mean curvature tensor, n^α is the tangential surface vector perpendicular to $\partial\Pi_i$, and Π_i is the support of ith basis function. In the case of a smooth surface, the last term on the right-hand side cancels with the adjacent surface patches. Thus, in this case, the normal components of the basis functions can be combined such that the divergence of the surface field is exactly zero. In the case of a non-smooth surface, the last term on the right-hand side does not cancel with the neighbouring surface patches and therefore must be computed explicitly. This requires using basis functions spanning a proper function space for the tangential field. Such basis functions are outside the scope of this paper and were not used in the present work.

V. CONCLUSIONS

We numerically tested a recently formulated surface integral equation method where the electric field and its normal derivative are chosen as the boundary unknowns. The preliminary results presented here are in agreement with the Mie series solution for both dielectric and lossy spheres. Furthermore, the method seems to be viable for numerical computations and may be further improved if we employ basis functions that enforce the continuity conditions.

REFERENCES

[1] A. J. Yuffa and J. Markkanen, "A 3-D tensorial integral formulation of scattering containing intriguing relations," *IEEE Transactions on Antennas and Propagation*, vol. 66, no. 10, pp. 5274–5281, Oct. 2018.

[2] J. DeSanto and A. Yuffa, "A new integral equation method for direct electromagnetic scattering in homogeneous media and its numerical confirmation," *Waves in Random and Complex Media*, vol. 16, no. 4, pp. 397–408, Nov. 2006.

[3] J. A. DeSanto, "A new formulation of electromagnetic scattering from rough dielectric interfaces," *Journal of Electromagnetic Waves and Applications*, vol. 7, no. 10, pp. 1293–1306, Jan. 1993.

[4] P. Grinfeld, *Introduction to Tensor Analysis and the Calculus of Moving Surfaces*, Springer, New York, 2013.

[5] S. Järvenpää, M. Taskinen, and P. Ylä-Oijala, "Singularity subtraction technique for high-order polynomial vector basis functions on planar triangles," *IEEE Transactions on Antennas and Propagation*, vol. 54, no. 1, pp. 42–49, 2006.

Johannes Markkanen received the D.Sc. degree in Electromagnetics from the Department of Radio Engineering, Aalto University, Espoo, Finland, in 2013. From 2014 to 2018, he was a Post-Doctoral Researcher with the Department of Physics, University of Helsinki, Helsinki, Finland. He is currently a Post-Doctoral Researcher with the Max Planck Institute for Solar System Research, Göttingen, Germany. His current research interests include computational methods in electromagnetics and thermophysics with an emphasis on planetary science applications.

Alex J. Yuffa received the B.Sc. degree (Hons.) in Mathematical and Computer Sciences, the B.Sc. degree (Hons.) in Engineering Physics, and the M.Sc. and Ph.D. degrees in Applied Physics from the Colorado School of Mines, Golden, CO, USA. In 2013, he joined the U.S. Army Research Laboratory, Adelphi, MD, USA, first as an ORAU PostDoctoral Research Fellow and then as a Physical Scientist. In 2016, he joined the National Institute of Standards and Technology, Boulder, CO, USA, as a Physicist. His research has been highlighted in *Optics and Photonics News magazine* and featured on the covers of *Optics and Photonics News magazine* and *Applied Optics journal*.

Joshua A. Gordon received the Doctorate degree in Optics and Electromagnetics from the College of Optical Sciences, University of Arizona, Tucson, AZ, USA. He is a Physicist in the Electromagnetics Division at the National Institute of Standards and Technology, Boulder, CO, USA. His current research areas investigate new technologies for electric field measurements which include robotic based antenna metrology systems, optical techniques for antenna alignment, and atom-based electric-field sensing.